JOURNAL OF CATALYSIS 8, 272–282 (1967)

The Kinetics of Hydrogen and Carbon Monoxide Oxidation over a Manganese Oxide

C. S. BROOKS

From the United Aircraft Research Laboratories, East Hartford, Connecticut

Received February 7, 1967; revised April 19, 1967

The oxidation of hydrogen and carbon monoxide over a catalytically active, highly defect manganese dioxide has been examined at temperatures between room temperature and 350°C employing chromatographic procedures. The heterogeneous oxidation rates for hydrogen and carbon monoxide in air for 48 000 to 52 000 ppm hydrogen and 36 000 to 45 000 ppm carbon monoxide were determined to be first order with respect to the hydrogen and carbon monoxide concentrations for the temperature range 96° to 290°C for hydrogen and 75° to 150°C for carbon monoxide. The depletive oxidation rates of hydrogen and carbon monoxide over this manganese dioxide at 1950 ppm hydrogen and at 3 to 6 vol % carbon monoxide were determined to be first order for essentially the same temperature range. The first order character of both the heterogeneous and depletive oxidation rates for hydrogen and carbon monoxide indicates that the reaction mechanism is a Rideal type and is due to coverage of most of the oxide surface with one of the reactive atomic (H) or radical (CO) species.

Introduction

Transition metal oxides used for catalysts in the air oxidation of combustible gases such as hydrogen and carbon monoxide are usually nonstoichiometric with highly defective structures. Various workers (*1–6*) have obtained evidence of the "active" or "mobile" character of at least a portion of the oxygen within the structures of these defect oxides. More recently Reinacker and Scheve (*7*) demonstrated a semiquantitative relationship between the catalytic activity of oxides of copper, manganese, cobalt, and silver for the oxidation of carbon monoxide in air at low temperatures (50°C) and the "active" oxygen associated with these metal cations in their higher valence states. Some recent measurements (*8*) have been made of the rates of depletive oxidation of hydrogen over a nonstoichiometric manganese dioxide at low temperatures (100° to 300°C) which suggest strongly that the depletive hydrogen oxidation rate is dependent upon a highly defect surface structure and oxygen "mobility" within the oxide lattice.

The present study consists of an examination of the kinetics of heterogeneous oxidation in air and of the depletive oxidation in nitrogen of low concentrations of hydrogen and carbon monoxide over a nonstoichiometric manganese dioxide. The principal objective of this study was to establish whether the kinetics of hydrogen and carbon monoxide oxidation are the same for the two reactants.

Experimental Procedure

Catalyst preparation and characterization. The manganese dioxide catalyst was prepared by precipitation from a solution of manganese nitrate by $NaClO_3$. Based on chemical composition and thermal decomposition history, the empirical composition of the freshly prepared oxide heated in air at temperatures lower than 200°C is $Mn_2O_3(OH)_2$. The manganese analyses estab-

TABLE 1
MANGANESE OXIDE STOICHIOMETRY

Catalyst portion	Oxygen content from neutron act. (wt %)	Mn oxide stoichiometry	
		Mn by chem. anal. and O by neutron activation	Mn by chem. anal. only (total Mn and Mn^{4+})
H-2-1-1	34	$MnO_{2.04}$	$MnO_{1.97}$
H-2-1-2	33	$MnO_{1.93}$	$MnO_{1.92}$
H-2-1-3	33	$MnO_{2.02}$	$MnO_{1.93}$
H-2-1-4	32	$MnO_{1.87}$	$MnO_{1.97}$
Average		$MnO_{1.97\pm0.07}$	$MnO_{1.95\pm0.02}$

lished that prior to depletive hydrogen oxidation 95% of the manganese is Mn^{4+} with the remainder being Mn^{3+}. Examination by X-ray diffraction indicated a highly disordered structure and permitted tentative identification with γ-MnO_2. Details of the preparation, chemical analyses, and rate measurements for heterogeneous oxidation of hydrogen in air and depletive oxidation of hydrogen are described elsewhere (*8*).

An additional analysis not previously reported consisted of an assay of the oxygen content by neutron activation analysis (General Atomic Division of General Dynamics). The oxygen so determined on the four manganese oxide preparations was reported to be accurate to 1%. The stoichiometry of the four oxide preparations calculated from the manganese determinations by chemical analysis and the oxygen determinations by neutron activation analysis are given in Table 1. The average composition of the four portions, based entirely on chemical analyses, was determined to be $MnO_{1.95\pm0.02}$, whereas the average composition based on the chemical analyses for manganese and the neutron activation analyses for oxygen was found to be $MnO_{1.97\pm0.07}$.

The BET nitrogen surface area of this manganese oxide was 0.59 m^2/g, and only in the case of oxide portions heated above 400°C did the surface area increase significantly above the reproducibility (30%) of the area measurements. The average particle size determined by photomicrograph was 0.69×10^{-4} cm. The photomicrograph particle size is sufficiently close to the average particle size of 1.02×10^{-4} calculated from the BET nitrogen area and the oxide density, assuming spherical geometry, to establish that there was essentially no internal porosity within the oxide crystallites.

Apparatus and test procedures. The apparatus and test procedures have been described previously (*8*). The measurements were all made employing continuous flow procedures in a microreactor with chromatographic analysis of the effluent gases from the catalyst bed. The hydrogen oxidation measurements were conducted with 116 mg of the manganese oxide (portion H-2-1-3) mounted on 11.320 g of Al_2O_3 (Norton SA 5101-⅛ inch pellets). The carbon monoxide oxidation measurements were conducted with 1 g samples of unsupported manganese oxide. The flow rates used were 45 ml/min at NTP for heterogeneous oxidation and 25 ml/min at NTP for the depletive oxidation. Transit times through the catalyst bed were of the order of 7 sec for the air oxidations and 12 sec for the depletive oxidations. The hydrogen was injected at concentrations of 38 000 to 52 000 ppm for air oxidation and mixed with nitrogen at a concentration of 1950 ppm for depletive oxidation. The carbon monoxide was injected at concentrations of 36 000 to 63 000 ppm for air oxidation and mixed with nitrogen at a concentration of 35 000 ppm for depletive oxidation. The conversion of hydrogen and carbon monoxide to oxidation products ranged between 0.2 and 0.7 for essentially all of the measurements. Pretreatment of the catalyst portions before each test run, unless otherwise indicated, consisted of passing air for 16 hr at 45 ml/min at NTP over the catalyst at 300°C.

Results

Heterogeneous Oxidation of Hydrogen and Carbon Monoxide in Air

Earlier work (*8*) established that the heterogeneous oxidation of hydrogen in air at hydrogen concentrations below 7 vol % at temperatures somewhat above room temperature to 300°C is first order with respect to the hydrogen concentration for the manganese oxide under consideration here. Oxidation of carbon monoxide in air at carbon monoxide concentrations in the range of 36 000 to 63 000 ppm at temperatures somewhat above room temperature to 150°C has been found to be first order with respect to the carbon monoxide concentration over this same manganese oxide.

A summary of the hydrogen and carbon monoxide oxidation in air for injection concentrations in the range of 36 000 to 52 000 ppm is given in Fig. 1 with the cumulative

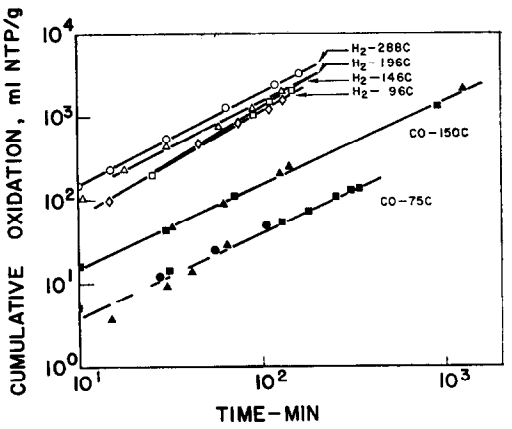

GAS	INJECTION CONCENTRATION	OXIDE PREPARATION H-2-I-1	H-2-I-2	H-2-I-3
H_2	48100-52200 PPM			○ △ □ ◇
CO	36400-45400 PPM	●	▲	■

Fig. 1. Oxidation of hydrogen and carbon monoxide in air at 75° to 300°C.

oxidation as ml NTP per gram of oxide vs. time in minutes. The oxidation rates for hydrogen exceed those for carbon monoxide. This is demonstrated in Table 3 and the section below comparing the oxidation coefficients for the two gases. However, the specific rate constants for carbon monoxide calculated from the first order dependence of the oxidation rates on reactant concentration exceed those for hydrogen. The low-temperature poisoning of oxidation sites in the case of carbon monoxide results in a larger slope, K, for the curve obtained for the oxidation rate plotted versus carbon monoxide concentration.

The specific rate constants for these hydrogen and carbon monoxide oxidation data at temperatures between 75° and 300°C are represented in Fig. 2. The activation en-

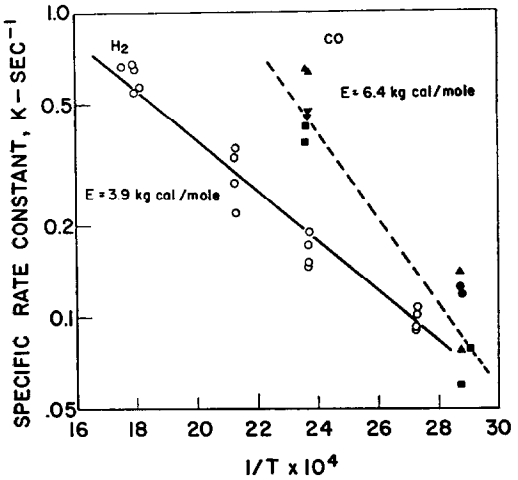

GAS	INJECTION CONCENTRATION	OXIDE PREPARATION H-2-I-1	H-2-I-2	H-2-I-3	H-2-I-4
H_2	48100-52200 PPM			○	
CO	36400-45400 PPM	●	▲	■	▼

Fig. 2. Hydrogen and carbon monoxide oxidation in air.

ergies calculated for the temperature dependence of the heterogeneous oxidation rates from the Arrhenius plot in this figure were determined to be 3.9 kcal/mole for hydrogen (*8*) and 6.4 kcal/mole for carbon monoxide. The somewhat greater variation in the rate constants at a given temperature for carbon monoxide compared to the hydrogen can be attributed to the fact that the data in Fig. 2 are for all four oxide portions for carbon monoxide, whereas only one oxide portion was used for the hydrogen.

Essentially complete loss of oxidation capacity occurs after equilibration at room temperature for 200 min at carbon monox-

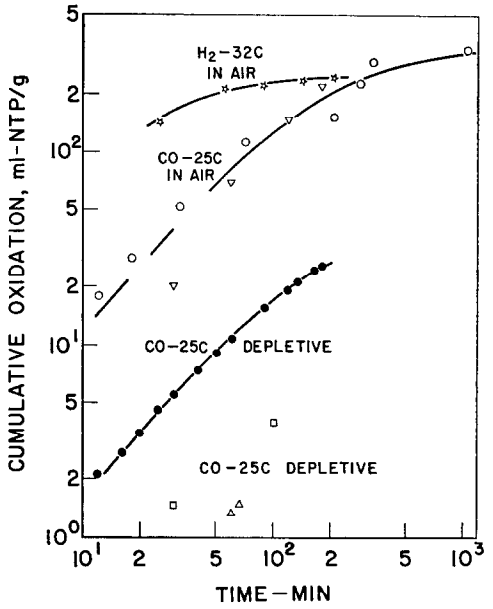

FIG. 3. Hydrogen and carbon monoxide oxidation at room temperature.

ide and hydrogen concentrations of the order of 36 000 to 63 000 ppm in air. This is illustrated in Fig. 3. The amounts of hydrogen and carbon monoxide oxidized at the end of 200 min exposure correspond to 10.9×10^{17} and 10.1×10^{17} molecules/cm^2, respectively, referred to the area of the manganese oxide as measured by the BET technique using nitrogen. An obvious conclusion that might be deduced from these saturation oxidation values is that they represent poisoning of the surface by retention of hydrogen and carbon monoxide oxidation products. This conclusion can be only partially correct, however, for the 10×10^{17} represents one thousand times the number of probable oxidation sites on the oxide surface estimated from crystallographic structural information (*9*). This suggests that, in addition to the poisoning of the surface with hydrogen and carbon monoxide oxidation products, another factor may be the gradual elimination of oxidation sites by assimilation of oxygen into the oxide to form the nearly stoichiometric manganese dioxide. Ordinary reagent grade manganese dioxide is approximately stoichiometric in composition and is devoid of oxidation catalytic activity (*8*).

The relatively large particle size (0.69×10^{-4} cm) of this manganese oxide and the absence of internal porosity indicate that diffusion effects should be negligible for these kinetic measurements. The unsupported oxide should have interparticle pores of dimensions comparable to the oxide particle size, i.e., $\sim 10^{-4}$ cm. The oxide supported on the alumina was deposited only on the outside surface of the pellets so that the intraparticle pores of the alumina pellet would not be involved in transport of reactant gases to the oxide particle surfaces. In estimates made of the role of diffusion in catalyst pore sizes, it has been pointed out by Wheeler (*10*) that for single-component gases diffusion effects are negligible at pressures less than 0.01 atm in pore sizes as large as 10^{-4} cm. In order to test for diffusion effects with the present gas mixtures the oxidation rates were determined as the flow rates were altered. Doubling the flow rates produced changes detectable within the accuracy of these rate measurements only for gas mixtures at the lowest reactant partial pressures ($\sim$2000 ppm) with either hydrogen or carbon monoxide. In the case of either the unsupported or supported oxide the ratio of the reactor tube diameter to the particle size is of the order of 600, so that radial concentration gradients should have a negligible effect on the observed oxidation rates.

Depletive Hydrogen and Carbon Monoxide Oxidation

The depletive oxidation reactions provide more insight into mechanisms than do the heterogeneous processes. A summary of the hydrogen and carbon monoxide depletive oxidation rate data for this manganese oxide for the temperature range $\sim$75° to 300°C appears in Fig. 6 of ref. (*8*) and Fig. 4 of this paper. The carbon monoxide data are presented as cumulative gas oxidized as molecules per cm^2 versus the time in minutes.

These data can be fitted satisfactorily to a first order kinetic expression, the integrated form of which is

$$2.3 \log_{10} [A/(A - X)] = K't + C \quad (1)$$

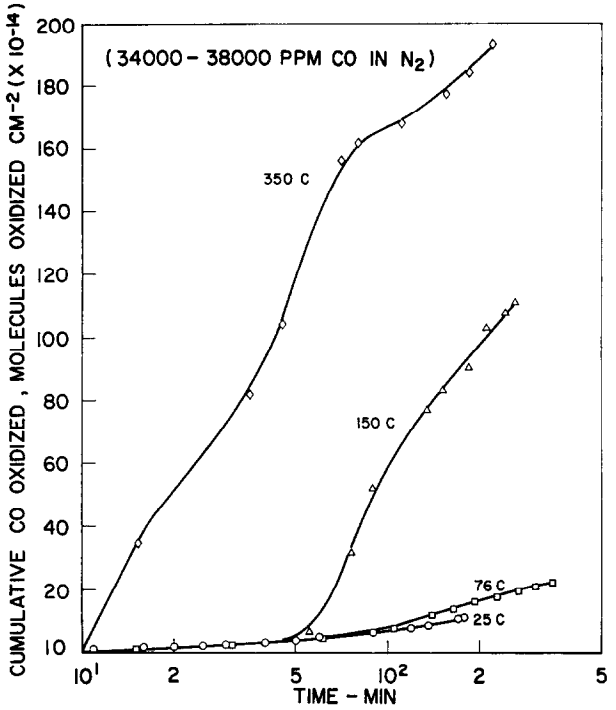

FIG. 4. Depletive carbon monoxide oxidation at 25° to 350°C.

where A represents the initial amount of manganese dioxide available for depletive oxidation, X represents the amount of manganese dioxide reduced to manganese monoxide at any time, t, and K' is the specific rate constant for the oxidation reaction. The depletive carbon monoxide oxidation data plotted in accordance with Eq. (1) are given in Fig. 5. The hydrogen data have been presented in Fig. 7 of ref. (*8*).

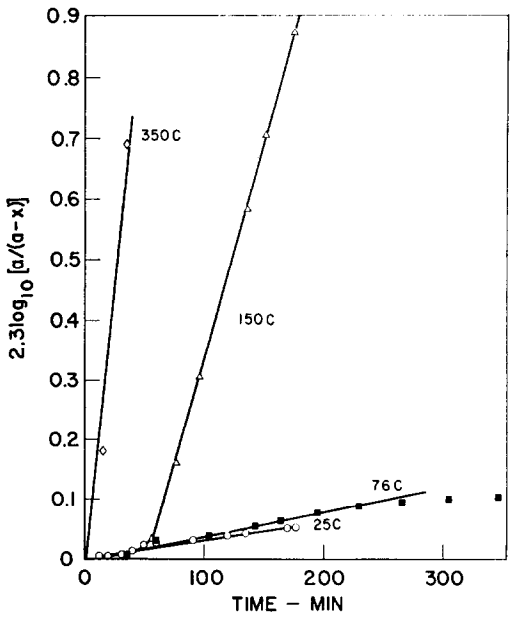

FIG. 5. Kinetics of depletive oxidation of carbon monoxide.

Other kinetic treatments were applied to the present depletive hydrogen and carbon monoxide oxidation data. One of the treatments consisted of an expression suggested by Prout and Tompkins (*11*) where the rate plots resemble a hyperbolic tangent function, and a maximum occurs in the depletive decomposition of an oxide around 50% depletion

$$2.3 \log_{10}\left[\frac{X/A}{(1 - X/A)}\right] = K''t + C_1 \qquad (2)$$

In the case of this treatment the data fit two linear curves, one at time less than 100 min and one at time greater than 100 min reaction time. In the case of the depletive carbon monoxide oxidation at 150° and 350°C the oxidation rate versus time definitely passes through a maximum around

TABLE 2
DEPLETIVE HYDROGEN AND CARBON MONOXIDE OXIDATION

Gas	Gas conc. (ppm)	Temp. (°C)	Time interval (min)	Specific rate constant K' Eq. (1) (sec^{-1})	Activation energy E' (kcal/mole)	Fraction MnO_2 converted to MnO at end of time interval
H_2	1950	100°	10–165	2.6×10^{-6}	3.7	0.027
		199°	165–435	16×10^{-6}		0.0248
H_2	1950	160°	10–220	5.1×10^{-6}	3.7	0.066
H_2	1950	210°	10–215	5.7×10^{-6}	3.7	0.0798
H_2	1950	264°	10–370	8.3×10^{-6}	3.7	0.17
H_2	1950	287°	28–389	17.8×10^{-6}	3.7	0.346
			389–770	24.6×10^{-6}		0.416
CO	34 000–38 000	25°	9–130	12.0×10^{-6}	5.0	0.094
CO	34 000–38 000	76°	12–200	15.3×10^{-6}	5.0	0.153
CO	34 000–38 000	150°	55–186	1.9×10^{-4}	5.0	0.875
			186–200			1.00
CO	34 000–38 000	350°	15–35	9.9×10^{-4}	5.0	0.424
			35–200			1.00

50% conversion of MnO_2 to MnO, but Eq. (1) is considered to have a better theoretical basis and to be more appropriate for application to the present data.

In order to examine the significance of these depletive oxidation data the rate constants calculated in accordance with Eq. (1) for hydrogen and carbon monoxide are given in Table 2. The Arrhenius plots of these rate constants are given in Fig. 6, and the activation energies calculated from the slopes of the Arrhenius plots are given in Table 2. Additional relevant information provided in that table is the fractional conversion of MnO_2 to MnO at the end of various time intervals. These results lead to the following conclusions:

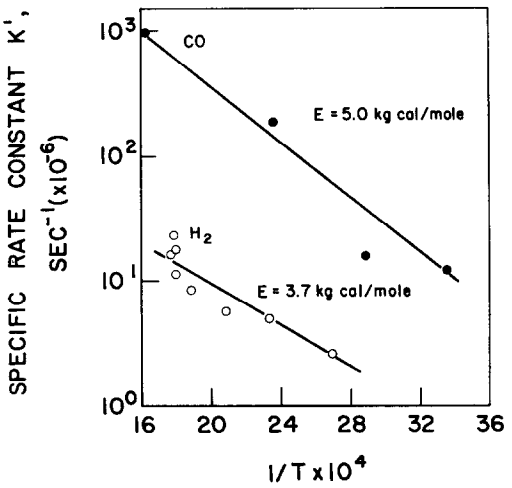

FIG. 6. Depletive hydrogen and carbon monoxide oxidation.

(1) The activation energy for the depletive carbon monoxide oxidation is 40% greater than that obtained for hydrogen.

(2) The activation energy of 3.7 kcal/mole for depletive hydrogen oxidation is in essential agreement with the value of 3.9 kcal/mole previously obtained for heterogeneous hydrogen oxidation over this oxide, whereas the activation energy for depletive carbon monoxide oxidation is 28% less than for heterogeneous carbon monoxide oxidation (Figs. 2 and 6). This close agreement in activation energies for the depletive and heterogeneous oxidations provides strong evidence that the presence of gas-phase oxygen in the heterogeneous process has a relatively minor effect upon the amount of carbon monoxide or hydrogen adsorbed on the oxide.

(3) A sharp inflection in the depletive carbon monoxide oxidation rate around 60 min at 150°C indicates the onset of an appreciable CO_2 desorption rate after an initial retention of chemisorbed carbon monoxide. No indication of carbon monoxide chemisorption occurs at 350°C, but strong retention occurs at 76°C and below.

The cumulative depletive carbon monoxide oxidation at room temperature of 25 ml NTP/g (see curve in Fig. 3) represents of the order of 100 monolayers of surface oxygen based on the surface oxygen concentration calculated from crystallographic structure of manganese dioxide. This means that a chemisorbed carbon monoxide monolayer represents little more than 1% of the saturation cumulative oxidation values for the depletive and no more than 0.1% for the heterogeneous carbon monoxide oxidation reactions at room temperature. In less than 10 min at room temperature with either hydrogen at 1950 ppm or carbon monoxide at 34 000 to 38 000 ppm sufficient exposure to reactive gas has occurred under the flow rates used to saturate the surface with chemisorbed hydrogen or carbon monoxide, providing adsorption is instantaneous. The several oxide preparations indicated by different symbols in Fig. 3 show marked differences in their room-temperature carbon monoxide oxidation rates, indicating the variable character of the low-temperature defect structure responsible for oxidation activity.

Oxidation Coefficients for Hydrogen and Carbon Monoxide Oxidation

The oxidation rates (σ) expressed as molecules per cm^2 per second and the oxidation coefficients (σ/n) for heterogeneous and depletive hydrogen and carbon monoxide oxidation are given in Table 3 for the temperature range of 25° to 350°C. The reactant concentrations all lie within the range of 45 400 to 52 200 ppm for the heterogeneous oxidations and within the range of 35 800 to 39 400 ppm reactant concentration for the depletive oxidations. The oxidation coefficient is defined as the ratio of the oxidation rate (σ) referred to unit surface area to the collision frequency (n) with the oxide surface of the given reactant at the indicated temperature and reactant partial pressure (P). The collision frequency with the oxide surface can be calculated from kinetic gas theory as

TABLE 3

OXIDATION COEFFICIENTS FOR HETEROGENEOUS AND DEPLETIVE HYDROGEN AND CARBON MONOXIDE OXIDATION OVER MANGANESE OXIDE

Reactant gas	Type oxidation	Reactant conc. (ppm)	Temp. (°C)	Time (min)	σ Oxid. rate (molecules cm^{-2} sec^{-1})	Oxidation coefficient (σ/n)	Mn oxide prep.
H_2	Heter.	51 900	96°	15	2.9×10^{15}	5.7×10^{-8}	H-2-1-3
				168	2.6×10^{15}	5.1×10^{-8}	
		52 200	146°	15	3.4×10^{15}	7.3×10^{-8}	H-2-1-3
				148	2.9×10^{15}	6.3×10^{-8}	
		48 100	196°	18	3.1×10^{15}	7.3×10^{-8}	H-2-1-3
				130	3.1×10^{15}	7.4×10^{-8}	
		49 100	288°	10	3.7×10^{15}	9.6×10^{-8}	H-2-1-3
				160	3.8×10^{15}	9.7×10^{-8}	
CO	Heter.	45 400	25°	30	3.5×10^{12}	2.6×10^{-10}	H-2-1-3
				102	2.5×10^{12}	1.9×10^{-10}	
		45 400	76°	30	3.9×10^{13}	3.2×10^{-9}	H-2-1-3
				325	2.9×10^{13}	2.4×10^{-9}	
		45 400	150°	30	11.8×10^{13}	10.5×10^{-9}	H-2-1-3
				70	12.1×10^{13}	10.8×10^{-9}	
CO	Depletive	39 400	25°	30	1.5×10^{13}	1.3×10^{-9}	H-2-1-1
				175	0.88×10^{13}	0.77×10^{-9}	
		39 400	76°	31	1.1×10^{13}	1.1×10^{-9}	H-2-1-1
				345	0.53×10^{13}	0.49×10^{-9}	
		39 900	150°	35	$< .5 \times 10^{13}$	$< .5 \times 10^{-9}$	H-2-1-3
				264	3.5×10^{13}	3.6×10^{-9}	
		35 800	350°	35	3.9×10^{14}	5.4×10^{-8}	H-2-1-3
				220	4.0×10^{13}	5.5×10^{-9}	

$$n = [3.52 \times 10^{22}(P)]/(MT)^{1/2} \quad (3)$$

where M is the molecular weight of the given gas component. The principal conclusions that can be drawn from these calculated parameters, σ and σ/n, are as follows:

(1) The heterogeneous oxidation coefficients for hydrogen change by factors no greater than 2, compared with factors of 4 to 10 for carbon monoxide for the 76° to 150°C temperature range.

(2) There are large differences between hydrogen and carbon monoxide for heterogeneous oxidation. At a given temperature such as 150°C for hydrogen, σ is at least thirty times that observed for carbon monoxide. The activation energies obtained demonstrate that the energy requirement for dissociative hydrogen adsorption is appreciably less than for molecular adsorption of carbon monoxide.

(3) In the case of carbon monoxide, σ/n is initially about four times greater for the depletive than for the heterogeneous oxidation at room temperature and only at temperatures of 76°C and above does σ/n for the heterogeneous oxidation exceed that for the depletive oxidation. This suggests that in the heterogeneous process at room temperature either there is strong competition of oxygen with carbon monoxide for adsorption sites or there are fewer oxygen vacancies which provide reaction sites.

(4) The differences in σ/n are considered more significant than differences in σ. In a comparison of the heterogeneous oxidation rates for hydrogen and carbon monoxide it is seen that σ/n for hydrogen exceeds that for carbon monoxide by a factor of about 25 at 76° to 96°C, whereas σ/n for hydrogen exceeds that for carbon monoxide by a factor of about 6 at 150°C.

(5) These kinetic data provide strong indirect evidence that the lower observed oxidation rates for carbon monoxide compared with hydrogen (notably at the lower temperatures) is due to loss of access to oxidation sites by chemisorbed carbon monoxide or retention of an oxidation product (CO_2, CO_3^{2-}).

Effect of Moisture on Carbon Monoxide Oxidation

Several claims (*12*, *13*) have been made that manganese oxide catalysts for carbon monoxide oxidation in air have been prepared so that they are insensitive to moisture. Duplication of these preparations and examination of their oxidation activity in air has not led to verification of these claims. In the case of the present manganese

TABLE 4

EFFECT OF MOISTURE ON CO OXIDATION IN AIR OVER MANGANESE OXIDE (H-2-1-4)

Reactant conc. (ppm)	Temp. (°C)	Time (min)	σ Oxid. rate (molecules cm^{-2} sec^{-1})	Oxidation coeff. (σ/n)	Pretreatment
62 500	25°	30	0.75×10^{14}	—	—
Dry		180	0.92×10^{14}	—	—
	150°	—	—	—	16-hr activation in Airflow
62 500	24°	30	1.17×10^{14}	—	—
8.95 mm Hg		180	0.28×10^{14}	—	—
H_2O V.P.	150°	—	—	—	1-hr activation in Airflow
62 500	149°	30	1.51×10^{14}	9.8×10^{-9}	—
14.2 mm Hg		180	1.50×10^{14}	9.8×10^{-9}	—
H_2O V.P.					
62 500	150°	15	2.22×10^{14}	14.4×10^{-9}	—
Dry		213	1.87×10^{14}	12.1×10^{-9}	—
62 500	26°	170	1.00×10^{14}	—	—
Dry					
62 500	26°	125	$< .01 \times 10^{14}$	—	—
8.95 mm Hg					
H_2O V.P.					

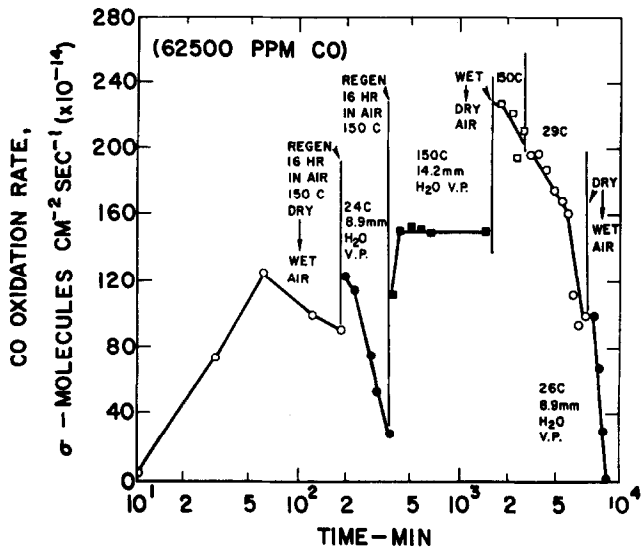

FIG. 7. Effects of moisture and temperature on CO oxidation activity in air.

oxide a series of tests was performed to establish the effect of moisture on the oxidation of carbon monoxide in air at room temperature and 150°C (Table 4 and Fig. 7). The oxidation rates (σ) and oxidation coefficients (σ/n) obtained in these tests demonstrate that rapid loss of oxidation activity occurs in 39% relative humidity (1.2 vol % of injected gases) at room temperature. Oxidation activity can be sustained but at reduced efficiency (a 30% reduction in σ/n) at 150°C in wet air (14.2 mm Hg water vapor pressure) compared with the oxidation activity in air predried over molecular sieves (Linde 5A) at —196°C. Further, it can be concluded that any losses in oxidation activity due to the presence of moisture are reversible and can be restored by heating in dry air at 150°C.

Reaction Mechanism

The observed first order kinetics for both the heterogeneous and depletive oxidation of hydrogen and carbon monoxide here indicate that the reactive surface of the oxide is essentially covered with a monomolecular layer of reactive species for the entire range of hydrogen and carbon monoxide concentrations examined. The mechanism suggested by Rideal (*14*) for catalytic ortho-para hydrogen conversion appears to be applicable. The following reactive species can be visualized for the heterogeneous oxidations:

$$2H\ (ads) + \tfrac{1}{2}O_2\ (g) \leftrightarrow H_2O\ (ads)\ \text{or}\ H_2O\ (g) \quad (4)$$

$$CO\ (ads) + \tfrac{1}{2}O_2\ (g) \leftrightarrow CO_2\ (ads)\ \text{or}\ CO_2\ (g) \quad (5)$$

The temperature determines whether or not the oxidation products remain adsorbed.

The mechanisms for the depletive oxidation reactions can be visualized as follows:

$$H_2\ (g) + O^{2-}\ (\text{lattice}) + 2\ Mn^{4+} \leftrightarrow H_2O\ (ads) + 2\ Mn^{3+} \quad (6)$$

$$CO\ (g) + O^{2-}\ (\text{lattice}) + 2\ Mn^{4+} \leftrightarrow CO_2\ (ads) + 2\ Mn^{3+} \quad (7)$$

The poisoning reactions for either the heterogeneous or depletive reactions can consist of retention of the reaction products, H_2O or CO_2, on the oxide surface at the lower temperatures. In addition, the following poisoning reactions can be visualized:

$$H_2\ (g) + 2O^{2-}\ (\text{lattice}) \leftrightarrow 2HO^-\ (\text{lattice}) \quad (8)$$

$$CO\ (g) + Mn^{4+}\ (\text{lattice}) \leftrightarrow CO\ (ads) + Mn^{4+}\ (\text{lattice}) \quad (9)$$

Based on crystallographic structural information on manganese dioxide (*9*), the maximum number of adsorption, if not reaction, sites would be of the order of 10^{15} per cm^2, if each surface ion (Mn^{4+} or O^{2-}) were to provide an adsorption site for either

hydrogen or carbon monoxide. Taking unit cell dimensions of $a_0 = 4.56$ Å, $b_0 = 10.70$ Å, and $c_0 = 2.85$ Å for an orthorhombic structure such as groutite, α-MnO(OH), in the absence of structural data on the present oxide, the surface concentration of the ions is calculated as the bulk concentration to the two-thirds power which for Mn^{4+} would be $(2.87 \times 10^{22})^{2/3} = 9.4 \times 10^{14}$ cm^{-2}, and for O^{2-} would be $(5.75 \times 10^{22})^{2/3} = 14.9 \times 10^{14}$ cm^{-2}. In view of the low order catalytic activity of stoichiometric manganese dioxide, it is more likely that the Mn^{3+} content of this catalytically active oxide indicates the magnitude of the defect structure providing reactive oxidation sites. In this case the initial surface concentration of oxidation sites would be of the order of one-twentieth of 10^{15} or 5×10^{13} cm^{-2}. This latter value is quite close to the concentration of oxygen vacancies of 2×10^{13} cm^{-2} estimated from the initial oxygen content based on neutron activation analysis.

Infrared examination of the oxide surface might be definitive in establishing the extent of HO^- and CO(ads) + Mn^{4+} chemisorption bonds formed during the oxidation process. The area available per oxidation site is of the order of 10×10^{-16} cm^{-2}, based on the above crystallographic estimates of the oxygen anion (O^{2-}) and the manganese cation (Mn^{4+}) surface concentrations. If Mn^{4+} were demonstrated to be the primary adsorption and oxidation sites for carbon monoxide, whereas O^{2-} were found to be the primary adsorption and oxidation sites for hydrogen, it would be very likely that poisoning of the oxide surface with chemisorbed carbon monoxide could leave unimpaired the adsorption sites for hydrogen. The present data do not provide any evidence for such performance, but evidence was obtained of such a phenomenon in the heterogeneous oxidation of hydrogen over a platinum oxide surface poisoned with chemisorbed carbon monoxide (unpublished experiments).

Oxygen Diffusion in Manganese Oxide

The kinetics of depletive oxidation of hydrogen and carbon monoxide appear to be primarily determined by the diffusion rate of the "active" or "mobile" oxygen within the manganese dioxide lattice. Oxygen diffusion coefficients were calculated from the rates of depletive oxidation of carbon monoxide over this oxide from an approximation to the solution of Fick's diffusion equations for desorption from a sphere with a uniform initial oxygen concentration, based on the treatment of Alberman and Anderson (*15*). The relation used for calculation of the diffusion coefficient is

$$\log_{10}(Y - Y_\infty) = \log_{10}[(6/\pi^2)(Y_0 - Y_\infty)] - (D_0 t/2.303R^2) \quad (10)$$

where Y is oxygen content at time t, Y_0 is the original oxygen content, and Y_∞ is the final oxygen content. This latter value corresponds to a manganese oxide composition of MnO. The effective spherical particle radius in cm is R and D_0 is the oxygen diffusion coefficient in cm^2 per sec. The total oxygen available for oxidation, $(Y_0 - Y_\infty)$, is taken as the oxygen which becomes available by reduction of Mn^{4+} to Mn^{++}. The initial Mn^{4+} was based on the chemical analysis of the freshly prepared oxide. D_0 was calculated from the slope $(D_0/2.303\,R^2)$ of the best line drawn through the linear portion of the plot of $\log_{10}(Y_0 - Y_\infty)$ vs. t. Linear curves were attained for depletive carbon monoxide oxidation after 20 to 60 min of operation.

Oxygen diffusion coefficients calculated from the depletive carbon monoxide oxidation data in Fig. 4 from Eq. (10) ranged from 5.5×10^{-14} cm^2/sec at 25°C to 1.4×10^{-12} cm^2/sec at 350°C. An examination of the literature shows that these calculated oxygen diffusion coefficients are surprisingly high compared with oxygen diffusion coefficients reported for other metal oxides at temperatures below 400°C. Only one uranium oxide (*16*) had a D_0 comparable to this manganese oxide at a comparable temperature.

The assumptions implicit in the application of Eq. (10) to these data include (1) particle shape is spherical, (2) there is a single particle size, and (3) the gas–solid reaction occurs exclusively at the particle surface. These conditions are not rigorously

met but they are considered to be approximated closely enough to make the estimate of the D_0 reasonably good. Photomicrographs show the oxide crystallites to be irregular in shape, but the ratio of the maximum to the minimum dimension is on the average less than 2. The average particle size established from photomicrographs of several portions was 0.69×10^{-4} cm with a size spread from 0.46×10^{-4} cm to 1.04×10^{-4} cm for one standard deviation. The principal assumption is that the rate-controlling process is primarily migration of lattice oxygen to the surface of the oxide particle. The assumption that reaction is limited exclusively to the gas–solid interface is considered reasonable, for molecular size would preclude appreciable penetration of the carbon monoxide into the oxide lattice.

The high order low-temperature mobility of the lattice oxygen in this manganese oxide is considered to dominate the kinetics of depletive oxidation of hydrogen and carbon monoxide. In addition, the "mobility" of the lattice oxygen is considered the key to the origin of the oxidation sites for the heterogeneous catalytic oxidation of these gases in air.

Acknowledgment

The author expresses appreciation to the United Aircraft Corporation for permission to publish.

References

1. Garner, W. E., *J. Chem. Soc.* (*London*), p. 1239 (1947).
2. (a) Garner, W. E., Gray, T. J., and Stone, F. S., *Proc. Roy. Soc.* (*London*) **197A**, 294 (1949); (b) Gray, T. J., *Proc. Roy. Soc.* (*London*) **197A**, 314 (1949).
3. Dell, R. M., and Stone, F. S., *Trans. Faraday Soc.* **50**, 501 (1954).
4. Jennings, T. J., and Stone, F. S., *Advan. Catalysis* **9**, 441 (1957).
5. Teichner, S. J., and Morrison, J. A., *Trans. Faraday Soc.* **51**, 961 (1955).
6. Elovich, S. J., *Proc. Intern. Congr. Surface Activity, 2nd, London* **2**, p. 252 (Butterworths, London, 1957).
7. Reinacker, G., and Scheve, E., *Z. Anorg. Allgem. Chem.* **330**, 27, 34 (1964).
8. Brooks, C. S., *J. Catalysis* **4**, 535 (1965).
9. Wyckoff, R. W. G., "Crystal Structures," Vol. I, 2nd ed., p. 292. Wiley, New York, 1963.
10. Wheeler, A., *Advan. Catalysis* **3**, 267 (1951).
11. Prout, E. G., and Tompkins, F. C., *Trans. Faraday Soc.* **40**, 488 (1944).
12. Katz, M., and Halpern, S., *Ind. Eng. Chem.* **42**, 345 (1950).
13. Pease, R. N., U. S. Patent No. 2,838,462 (June 10, 1958).
14. Laidler, K. J., "Chemical Kinetics," Chap. 6. McGraw-Hill, New York, 1950.
15. Alberman, K. B., and Anderson, J. S., *J. Chem. Soc., Suppl. Issue No. 2*, p. S303 (1949).
16. Aronson, S., Roof, R. B., and Belle, J., *J. Chem. Phys.* **27**, 137 (1957).